EEET ECOLOGICAL ENGINEERING & ENVIRONMENTAL TECHNOLOGY

Ecological Engineering & Environmental Technology 2024, 25(5), 42–60
https://doi.org/10.12912/27197050/184320
ISSN 2719-7050, License CC-BY 4.0

Received: 2024.02.10
Accepted: 2024.03.14
Published: 2024.04.01

Mapping Environmental Impacts in North-Western Algeria through Multivariate Spatio-Temporal Analysis Using Remote Sensing and Geographic Information System

Ikram Mahcer[1*], Djelloul Baahmed[1], Cherifa Hanene Kamelia Chemirik[1], Rachid Nedjai[2]

[1] Civil and Environmental Engineering Laboratory (LGCE), Hydraulic Department, Faculty of Technology, University of Djillali Liabès, 22000 Sidi Bel Abbes, Algeria

[2] CEDETE Laboratory EA 1210, University of Orleans, 10 Rue de Tours, 45069 Orléans, France

* Corresponding author's e-mail: ikrammahcer13@gmail.com

ABSTRACT

The interactions between the normalised difference vegetation index (NDVI), the normalised difference built-up index (NDBI), and land surface temperature (LST) are complex. The assessment of land use/land cover (LULC) changes in the North-western region of Algeria between 1995 and 2021 confirms the direct influence of these factors on surface thermal processes. The use of new information technologies, particularly remote sensing coupled with GIS, favourably contributes to the processing of a large volume of data and to the use of specific methods aimed at confirming and/or disproving the hypotheses put forward. The application of LULC classification methods clearly highlights the magnitude of transformations, predominantly in favour of intensified urbanisation over the past two decades. Indeed, agricultural lands have experienced a reduction of 17.45%, while urbanised areas have nearly doubled. This phenomenon can, in part, be attributed to the mass migration of populations from inland areas to the coast, not only due to climate change: secondary for political problems between 1990 and 2001. Similarly, barren lands have increased by 10.45%. These changes have real implications for ecosystems (mainly loss of biodiversity) and the climate (pollution, GHG emissions, and rising ambient temperatures). The estimation of average LST from multiple satellite scenes reveals an increasing trend, rising from 36.6 °C in 1995 to 40.35 °C in 2021. The direct relationship between LST and NDVI and between LST and NDBI confirms the close association between land use change and increasing surface temperatures. The Pearson coefficient between LST and NDVI showed a negative correlation, ranging between -0.52 and -0.47, while it was positively correlated between LST and NDBI, with values around 0.66. The emergence of hotspots in the region, confirmed by the results of analysis employing the Getis-Ord G* method, is marked by clearly increasing spatial envelopes. This phenomenon is associated with a distinct reduction in vegetation cover density, coupled with an increased vulnerability to drought conditions. These initial results argue in favour of preserving green and blue networks and, more largely, ecosystems.

Keywords: remote sensing, GIS, GEE, climate change, NDVI, NDBI, LST, Algeria.

INTRODUCTION

The last two decades (2001–2020) have witnessed a marked increase in global surface temperatures (0.99 °C on average) (Masson-Delmotte et al., 2021). Forecasts for the end of this century indicate a significant rise in these same temperatures, varying between 1.1 and 6.4 °C (IPCC, 2022). This climate warming has already profoundly altered the structure and functioning of terrestrial ecosystems to varying degrees, creating heterogeneity on a global scale (Müller and Bahn 2022). More locally, in Algeria, the north-western region is situated in a transitional zone between an arid and semi-arid climate. This climatic situation directly exposes the region to the impacts of climate change. The thermal effects and associated processes (evaporation, drought, low and/or intense but short-duration precipitation, etc.) highlight the high variability of temperatures across the territory.

The north-western region of the country is particularly affected by extreme climatic events as well as prolonged periods of drought (Bentchakal et al., 2021). Accordingly, considerable economic and social challenges as well as stress on the natural environment are prevalent. In order to address these climate warming-related issues, the use of new information technologies (GIS, remote sensing (RS)) has proven to be crucial for several reasons, namely: the development of new land cover classification algorithms, the processing of large volumes of data (images, etc.), and the integration of thermal calculation methods within these GIS tools (Ghai and Kumar 2021). Satellite imagery, with its improved resolution, serves as an unequivocal barrier for monitoring temporal changes in numerous environmental parameters. Furthermore, it is now possible to obtain cost-effective and replicable synoptic coverage over large regions (Atayi et al., 2016; Sudhakar and Reddy 2022). The importance of RS and GIS in the spatiotemporal monitoring of land in the Northwest of Algeria, particularly in the context of tracking land surface temperature (LST), normalised difference vegetation index (NDVI) and normalised difference built-up index (NDBI), is of paramount importance. These technologies offer valuable information on land cover changes, environmental dynamics and their interconnection with key indices (Keerthi Naidu and Chundeli 2023).

LST and NDVI are essential indicators for assessing climate change, acquiring climate trends and monitoring plant growth (Fayech and Tarhouni 2021; Malik et al., 2019; Naserikia et al., 2019).These two parameters serve as crucial indicators, making it possible to discern a wide range of environmental and terrestrial changes on a regional and global scale (Abdulmana et al., 2021; S. Li et al., 2021). Thermal infrared (TIR) bands are used to identify the relationships between LST and NDVI using RS techniques (Ghobadi et al., 2015; Hasan et al., 2022; Kumari et al., 2018). However, NDVI is commonly used to monitor the interaction between LST and vegetation, while NDBI is used to assess the degree of urbanisation (Bhatti and Tripathi 2014; Ferrelli et al., 2018; Sharma et al., 2015; Zhang et al., 2017). Many studies have explored the complex relationships between LST and established spatio-temporal correlations of indices (NDVI, NDBI) (Alademomi et al., 2022; Guha et al., 2021; Keerthi Naidu and Chundeli 2023). The studies examining the relationship between LST and soil indices frequently reveal a positive correlation between NDBI and LST and a negative association between NDVI and LST (Hasan et al., 2022; Macarof and Statescu, 2017; Zheng et al., 2021). Furthermore, in urban areas, some scientists have observed a particularly strong negative correlation between NDVI and NDBI (Shahfahad et al., 2020; Zeren Cetin et al., 2023). The vegetation health index (VHI) is a remote sensing index used to monitor and assess the impact of drought on vegetation. VHI has been used in various studies to analyse drought and vegetation dynamics, making it a valuable tool for assessing vegetation health in different regions (Ayad et al., 2023)

Additionally, understanding the dynamics of LULC changes is crucial for effective urban planning and environmental management. By continually monitoring these changes, policymakers and urban planners can make informed decisions to mitigate the environmental impacts of urbanisation and promote sustainable development. This is particularly important given the irreversible effects of LULC changes on the environment, such as the intensification of urban microclimates and associated implications for ecosystems (Policelli et al., 2018; Tayeb and Kheloufi 2019; Hussain et al., 2020). Multitemporal satellite images have been sparingly employed in the planning and monitoring of LULC changes in semi-arid and arid environments (Roy and Inamdar 2019; Yonaba et al., 2021). However, effective LULC mapping is achieved through the use of satellite imagery that provides a broad spectrum of spatial and temporal resolutions (Aredehey et al., 2018; Akhsin et al., 2024). There is a complex relationship between LULC changes, LST and soil indices (Alademomi et al., 2022; Ferrelli et al., 2018; Zhang et al., 2017).

To understand the physical processes that regulate and control the aforementioned factors, the objectives of this analysis were aimed at assessing the complex dynamics and interrelationships that exist among the environmental variables NDVI, NDBI, LST, and LULC using multispectral Landsat images. These may also be essential for adaptation and remediation in the face of the impacts of climate change. The objectives are fivefold: (1) mapping and evaluating LULC change patterns over 26 years, (2) determining LST using Landsat thermal bands and spectral indices NDVI and NDBI, (3) mapping, analysing, and detecting changes in LST, NDVI, and NDBI; (4) evaluating the correlation between LST, NDVI, and NDBI and their relationship

with changes in land cover; (5) identifying the regions particularly vulnerable to drought using GIS tools and NDVI-VHI indices, enabling targeted mitigation and resource allocation.

Study area

Located in the north-western region of Algerian territory (Figure 1), the study area fully encompasses two major watersheds: Tefna and Macta, situated in the Tlemcen and Sidi Bel Abbès departments, respectively (Table 1). The climatic characteristics observed within the two watersheds are similar to the predominant climate in the Mediterranean region of North Africa, characterised by a semi-arid climate pattern with rainfall in winter and drought conditions in summer. This distribution directly influences the availability of water in the watersheds, posing challenges for water resource management and the ecology of the region.

MATERIALS AND METHODS

Data collection and processing

Data sources are diverse and manifold, involving both internal data generated by organisations located within the study area and external, often referred to as contextual data, produced by national and/or international entities. The first type of data was used to validate the results of calculations based on indirect acquisitions, while the second was used to highlight the regional and/or global nature of thermal phenomena and eliminate scale effects.

The satellite data employed in this study originated from the LANDSAT 5 TM satellite missions (1995, 2000, 2005 and 2010), as well as LANDSAT 8 OLI (2015 and 2021). These images were acquired during the month of August (Table 2). The scenes corresponding to these different time periods were downloaded from the USGS

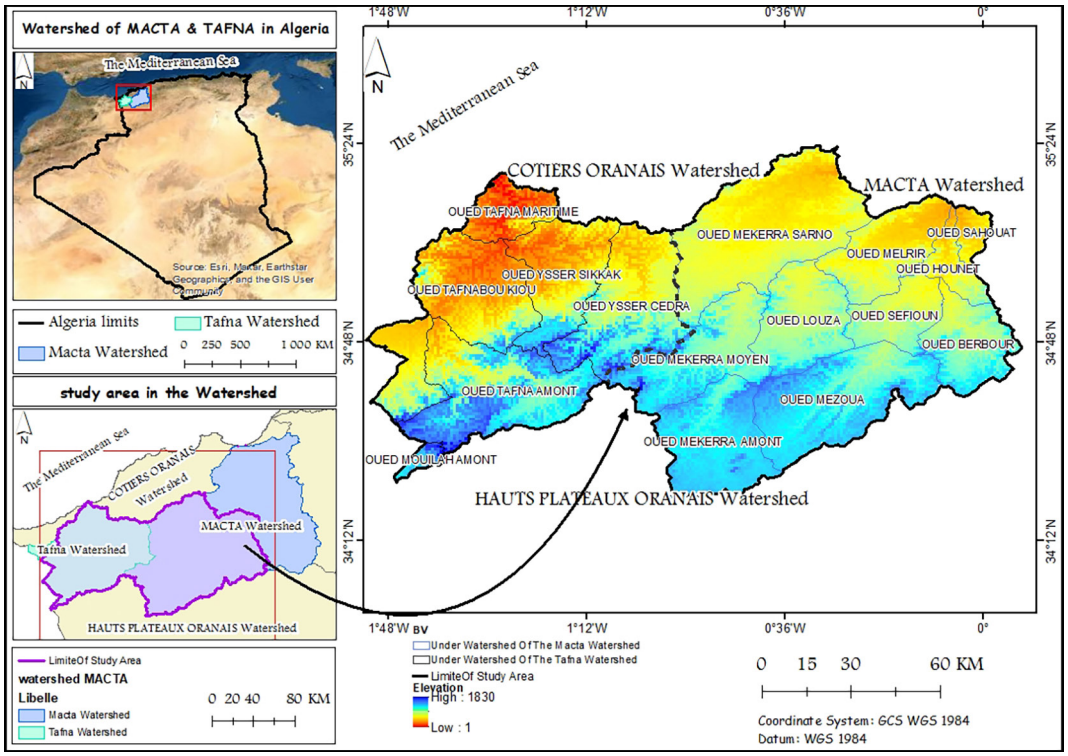

Figure 1. Location of study area

Table 1. Hydroclimatic characteristics of the catchment areas

Watershed	Lat.	Long.	Area	Perimeter	Alt. Min	Alt. Max.	Kc
Tafna	34°47 35°10	-2° 1°	5335	437	100	1810	1.69
Macta	34° 28' 35° 87'	0° 52' 1° 2'	14406	724	-10	1600	1.69

Table 2. Properties of Landsat images used

Satellite	Bands	Band width (µm)	Resolution (m)	Dates
LANDSAT 5	Band 3 Red	0.63-0.69	30	28 August1995 09 August2000 23 August2005 05 August 2010
	Band 4 NIR	0.76-0.9	30	
	Band 5 SWIR1	1.55-1.75	30	
	Band 6 SWIR 1	-	60	
LANDSAT8	Band 4 Red	0.64-0.67	30	18 August2015 18 July 2021
	Band 5 NIR	0.85-0.88	30	
	Band 6 SWIR 1	1.57-1.65	30	
	Band 10 TIR 1	10.6-11.19	100	
	Band 11 TIR 2	11.5-12.51	100	

database (Kumari et al., 2018). The choice of August is based on the objective of obtaining satellite imagery data of excellent quality to minimise the possible disturbances caused by atmospheric factors such as clouds. Table 2 describes the principal characteristics of the images used.

Despite the selection of high-quality satellite images, atmospheric correction is a critical step in the preliminary processing of RS data. Its essential role is to minimise or eliminate undesirable the atmospheric disturbances (atmospheric corrections, especially for temporality) mentioned above, which is fundamental to ensuring that accurate information is obtained about the Earth's surface (Lhissou et al., 2020). The FLAASH (fast line-of-sight atmospheric analysis of spectral hypercubes) model was used for image pre-processing due to its capacity to correct the spectral properties of light over a broad range, covering from visible light to 3 µm, including the near-infrared (NIR) and short-wave infrared (SWIR) regions. This correction requires prior radiometric calibration of the image, along with contextual data (flight date, departure time, GMT, geographical position of the scene centre, sensor altitude, and ground elevation) (Rani et al., 2017). The reflectance values obtained will be used to calculate the various indices.

Remote sensing indicator

The NDVI and NDBI indices provide crucial information on the distribution of vegetation and urban development, respectively. Together, NDVI and NDBI offer a valuable perspective on the interactions between natural ecosystems and urbanised areas and precise information on soil temperatures in particular and associated processes (evaporation, infiltration, etc.) (Fayech and Tarhouni 2021; Guha et al., 2021). LST is an essential indicator, revealing climatic variations and eventual temperature increases (Ferrelli et al., 2018; Kumari et al., 2018; Malik et

Table 3. Formula for calculating indices

Indices	Equation	Description
NDVI	$NDVI = \frac{(NIR-RED)}{(NIR+RED)}$ Eq. (1)	where: NIR is the near infrared band and Red is the red band
NDBI	$NDBI = \frac{SWIR-NIR}{SWIR+NIR}$ Eq. (2)	SWIR: short-wave infrared bands, NIR: near infrared
VHI	VHI=0.5×(VCI+TCI) Eq. (3)	VCI = (NDVI - $NDVI_{min}$) / ($NDVI_{max}$ - $NDVI_{min}$) TCI = (T_{max} - T) / (T_{max} - T_{min})
Steps in calculating LST: 1.Converting the satellite's digital number to Radiance 2.Conversion of radiance to sensor temperature 3.CalculatingEmissivity(ελ)	1.Lλ=ML×Qcal+AL-Oi Eq. (4)	Lλ: radiance, ML: multiplicative rescaling factor, Qcal: band 10 image, AL: additive image and Oi is the band 10 corrections
	2.BT = K2/ln [(K1 / Lλ) + 1] - 273.15 Eq. (5)	BT: brightness temperature, K1 and K2: the band-specific thermal conversion constants from the metadata, where: $K1$ = 774.883.09, $K2$ = 1321.0789(Fabeku et al., 2018)
	3.ελ = 0.004Pv + 0.986 Eq. (6)	Pv: proportion of vegetation (fraction of vegetation cover), based on a standardised NDVI value for each pixel
	LST = BT / [1 + λ × (BT / ρ) × ln(ελ)] Eq. (7)	λ: wavelength of the emitted radiance (λ = 11.5 µm), ρ = 1.438 × 10^{-2} mK

al., 2019). The vegetation health index (VHI) provides a comprehensive assessment of vegetation health and temperature conditions, and its valuable information on vegetation health and temperature conditions helps to assess and monitor drought conditions (Zeng et al., 2022). VHI is a composite index that combines vegetation condition index (VCI) and temperature condition index (TCI) derived from satellite data. In the presented study, VHI can be useful for identifying the regions vulnerable to drought.

Methodology

The calculation was carried out by taking the average of the data for all cloud-free pixels (0–5%) in August during the study period. This approach helps minimise any influence, from outliers or specific local conditions. To explore the relationship between the different parameters analysed, the diagram (Figure 2) shows the approach applied in the conducted processing (Alademomi et al., 2022). LULC is calculated by the Google Earth Engine (GEE) platform and a JS script was developed to collect Landsat images comprising multiple bands. Complete coverage of the study area was provided by a mosaic of 5 scenes (Feizizadeh et al., 2023). The LULC model is characterised by four classes: vegetated area (forest and agriculture), built-up area, bare land, and water bodies in the study area. The supervised classification schema were applied to temporal satellite datasets for six years 1995, 2000, 2005, 2010, 2015 and 2021, then exported from GEE to ArcGIS to generate the final maps.

*Identifying significant spatial clusters using Getis-Ord Gi**

Analysis Getis-Ord Gi* statistics is a spatial statistical analysis method frequently used in spatial analysis and GIS in general. Its aim is to identify the places with a high (hot spots) or low (cold spots) concentration of data by aggregating observation points into polygons based on calculated distances. This approach generates Z scores (Gi scores) and P values (Gi P values) for each

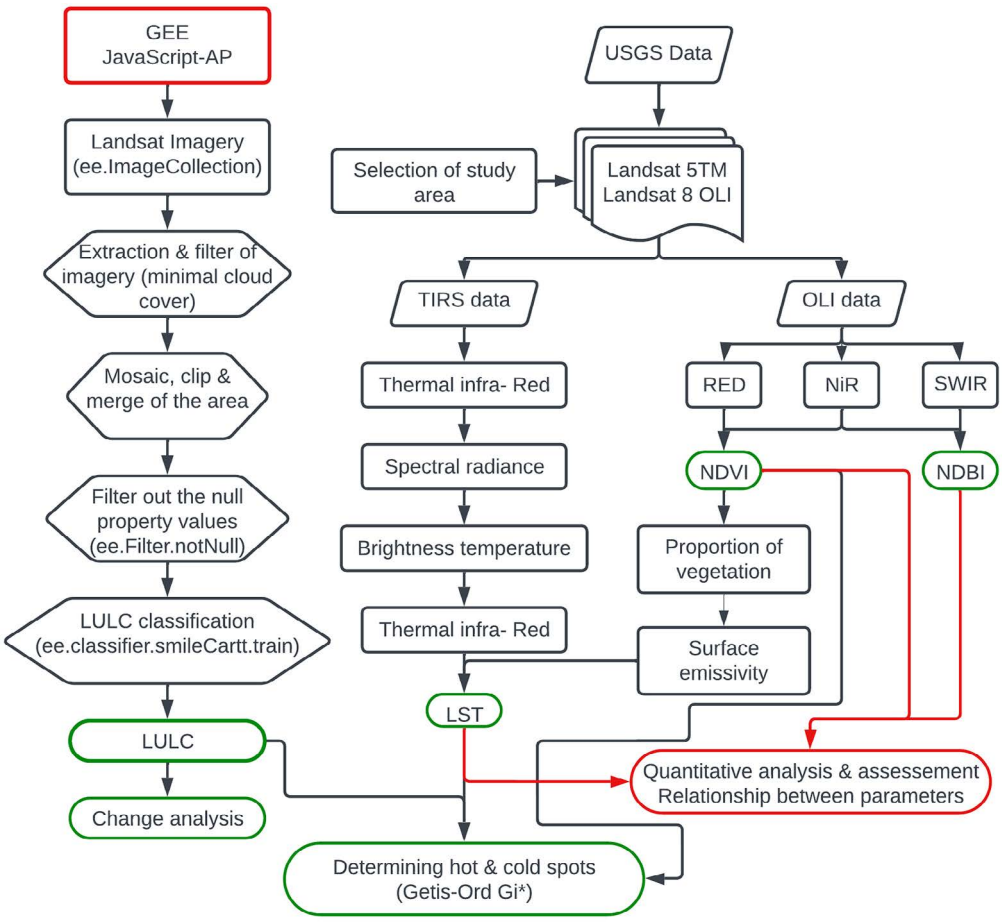

Figure 2. Methodological diagram used to calculate satellite indices

entity, making it possible to determine whether they belong to a group of high or low values compared with their neighbouring entities (Rossi and Becker 2019). Applying the Getis-Ord Gi* statistics to the NDVI and LST datasets makes it possible to identify significant spatial groups and hotspots related to vegetation density and temperature variations.

LULC and LST predictions for 2030 and 2050

The QGIS tool MOLUSCE and the cellular automata (CA) model are used to predict LULC and LST for the years 2030 and 2050. Two types of data are used to produce this prediction: dependent variables, like changes in LULC and estimated LST using a transition matrix from Landsat images taken in 1995 and 2005; and independent variables, like NDVI and NDBI. Landsat images are scaled using average aggregation rules to make the spatial resolution more consistent. The resampling function in ArcGIS makes this process easier (Mehmood et al., 2023). LST data are classified into six distinct temperature zones to provide an overview of temporal and spatial variations between LST zones. These zones are defined as very cold (<21.1 °C), cold (21.1 – <23.1 °C), chilly (23.1 – <25.1 °C), cool (25.1–27.1 °C), warm (27.1–29.1 °C); hot (29.1 – <31.1 °C) and very hot (> 31.1 °C) (Purwanto et al., 2016). After classification, each LST zone is superimposed on the LULC change maps, and LST variations are quantified using ArcGIS 10.8 "Tabulate Area" tool. The transition potential matrix is constructed using the above variables. During the prediction model training process, parameters such as the maximum iteration (set at 1,000). When modelling the transition potential matrix using an artificial neural network, in particular a multilayer perceptron (MLP), the simulation step produces potential transition maps, a certitude function (of an experimental nature) and prediction results for years 2030 and 2050. To guarantee the model's reliability in projecting the LULC and LST changes for a specified forecast year, model validation is deemed necessary and carried out using current datasets (Edan et al., 2021; Santos et al., 2021). Therefore, before projecting changes for 2030 and 2050, a rigorous accuracy assessment is carried out by simulating LULC and LST for the year 2021, and then comparing them with LULC and LST estimates for the same year. The QGIS-MOLUSCE validation module is used to calculate the overall kappa coefficients and percentage accuracy of the projected LULC and LST maps for year 2021. Once a satisfactory level of accuracy has been established, the model is applied to the final projection of LULC and LST for the forecast targets.

RESULTS AND DISCUSSION

Spatial detection of LULC changes

According to (Figures 3 and 4), the north-eastern part of the study area underwent rapid urbanisation between 1995 and 2021, resulting in a considerable reduction in forest to the profit of urban areas. Only the south-western parts of the Tafna area have conserved a certain amount of vegetation. By 2010, the areas dedicated to agriculture and forests had decreased, resulting in an increase in bare soil of 10.45%. The year 2021 was marked by a significant change, with a notable decrease in agricultural areas of around 17.45%; this observation is the formal translation of a gradual abandonment of cultivated land in favour of urbanised areas for a large part and probably left fallow for a small part. These observations highlight the significant changes in the spatial distribution of the various LULC classes in the study area. Rapid urbanisation has led to a reduction in green areas. In addition, the green zone, which includes natural areas and woodlands, recorded a very significant decrease over the study period, from 19.69% in 1995 to 14.11% in 2010 (Figure 4).

A 10.34% reduction in agricultural land between 2015 and 2021 (Figure 4) in favour of urban areas and bare soil, representing a significant change in land use patterns. The water class saw a reduction of 11.31% over the same period, highlighting the severe and repeated droughts that have occurred over the last two decades. They indicate the potential deterioration of resources under the dual effect of pumping and surface withdrawals from water courses, leading to a low level of available stocks. At the same time, a significant increase of 8.63% in bare soil was recorded, caused by land clearance and/or linked to changes in land management practices. Urban areas, with a 13.97% increase in surface area, stand out clearly from the other themes, confirming continued and rapid urban expansion, resulting in urbanisation pressures and a substantial decrease in land. Forest areas show very clear fluctuations. In fact, there was a decrease between 1995 and

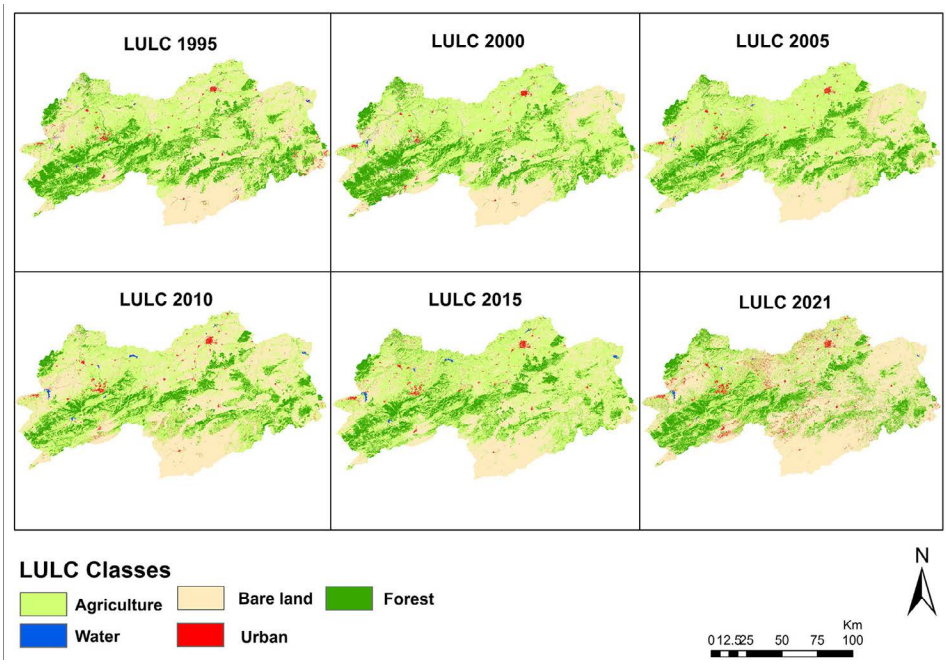

Figure 3. LULC maps for the study period

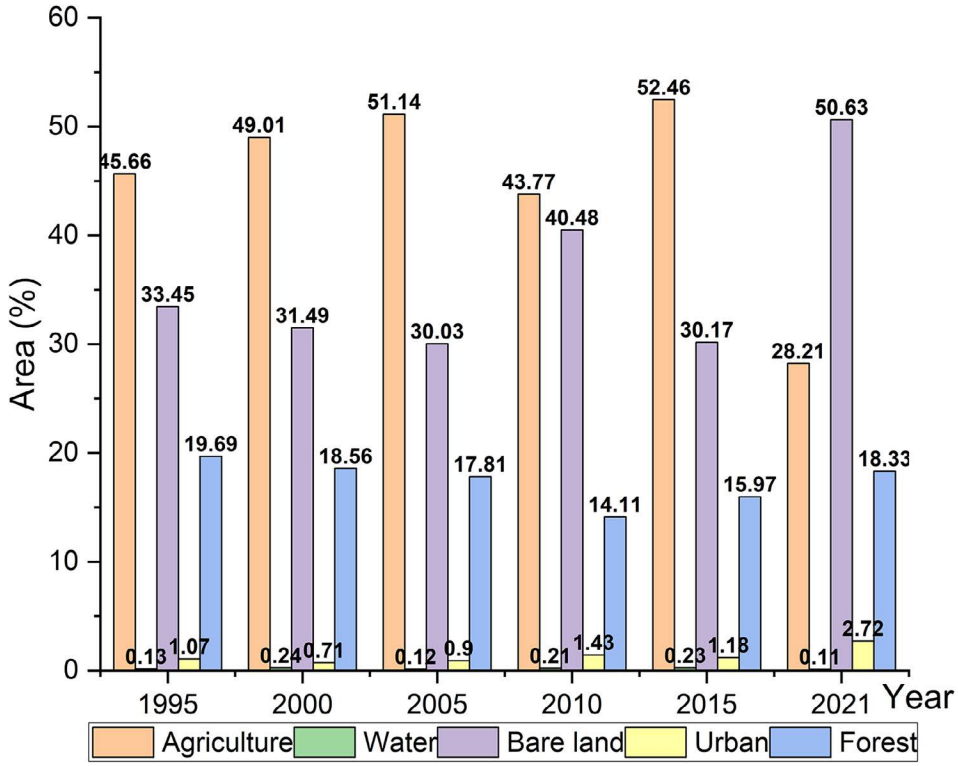

Figure 4. LULC areas of the different classes

2010 (-4.66%), suggesting deforestation and/or forest degradation (forest fires, cutting, etc.). Conversely, between 2010 and 2021, an increase in forest area of 2.30% indicates a recovery or stabilisation of forest cover because of the government's policy of protecting and preserving the forest patrimony.

Analysis of changes to the LST

The spatial representation of LST reveals a distinct thermal zoning (Figure 5). The maximum temperatures recorded during the respective years (1995, 2000, 2005, 2010, 2015, and 2021) were 49.56 °C, 50.28 °C, 47.39 °C, 54.17 °C, 40.22 °C,

Table 4. The rate of change in LULC over the different periods

Transition rate of change in LULC (%)					
Classes	1995–2000	2000–2005	2005–2010	2010–2015	2015–2021
Agriculture	1.41	0.85	-3.11	3.62	-10.34
Water	11.78	-13.22	10.88	1.47	-11.31
Bare land	-1.21	-0.95	5.98	-5.88	8.63
Urban	-8.12	4.73	9.19	-3.90	13.97
Forest	-1.18	-0.82	-4.66	2.48	2.30

and 49.86 °C, while the corresponding minimum temperatures were 12.36 °C, 18.38 °C, 15.64 °C, 21.06 °C, 21.17 °C, and 23.67 °C. An analysis of the 26 year study period reveals an increase in the minimum ground temperature of 11.31°C, accompanied by a marginal increase of about 0.3 °C in the maximum temperature. Notable extremes were observed in 2010 and 2021, with the highest and lowest LST values reaching 54 °C and 12 °C, respectively. Urban areas displayed the highest temperatures, while vegetated zones exhibited the lowest temperatures. This situation is a result of unregulated urbanisation practices (soil sealing, lack of green and blue screens, a growing number of cars, water stress on plants, etc.). This pattern is evident in (Figure 5 and 6) suggesting a distinct relationship between the types of LULC and the distribution of LST.

Analysis of variation in NDVI and NDBI

The spatio-temporal distribution of NDVI and NDBI over the period 1995–2021 is presented in (Figures 6 and 7). Figure 6 illustrates the average NDVI values for the study period. The derivation of NDVI in the north-western region of Algeria has revealed pronounced spatio-temporal variability in vegetation. The south-western parts of Tefna and Macta show high NDVI values, indicating abundant vegetation cover, consisting essentially of forests. Regionally, there was a decrease in mean NDVI in 1995, while NDVI values substantially increased from 2000 to 2010. From 2015 to 2021, the progression notably decreased, accompanied by a sharp decline in average NDVI values (Figures 4 and 6). The NDBI maps in (Figure 7) clearly highlight a significant increase in

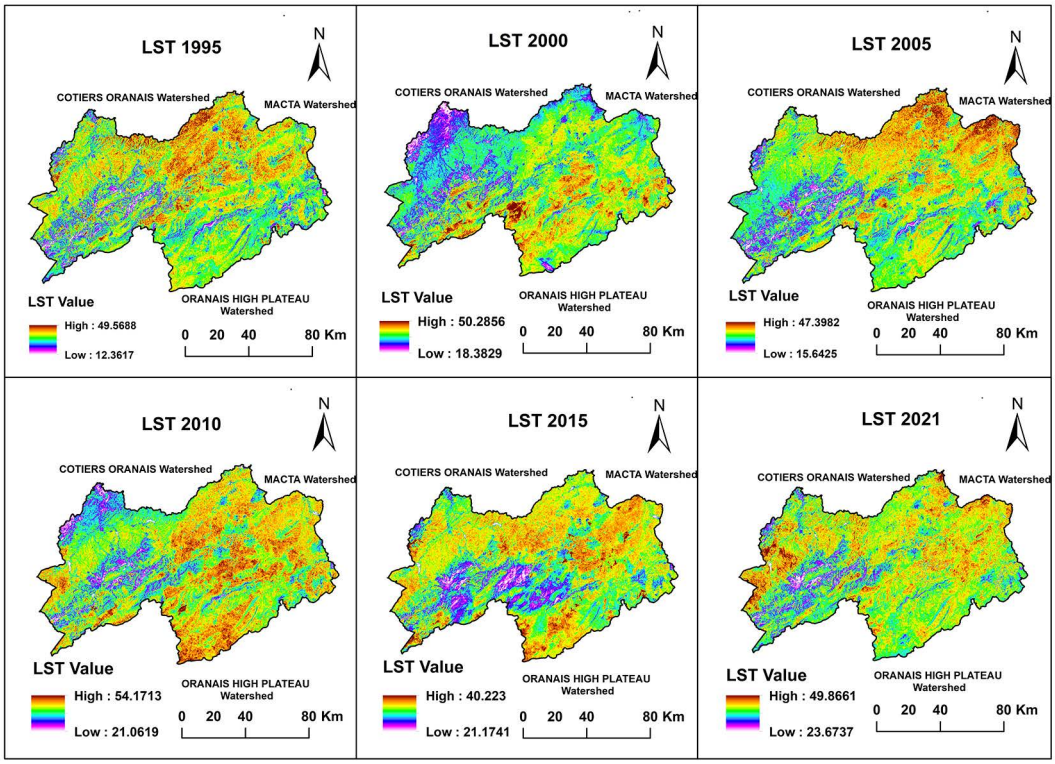

Figure 5. Spatial and temporal variation in LST over the period studied

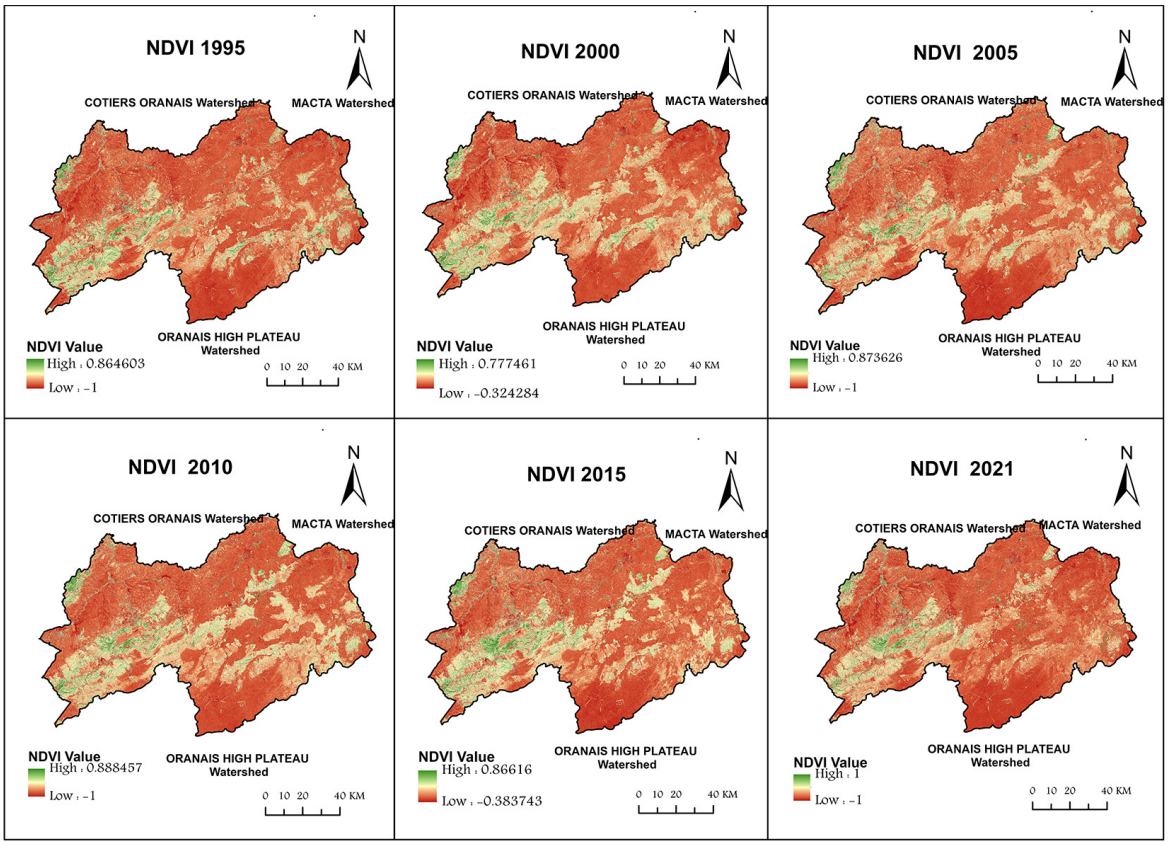

Figure 6. Spatiotemporal variation of NDVI during the study period

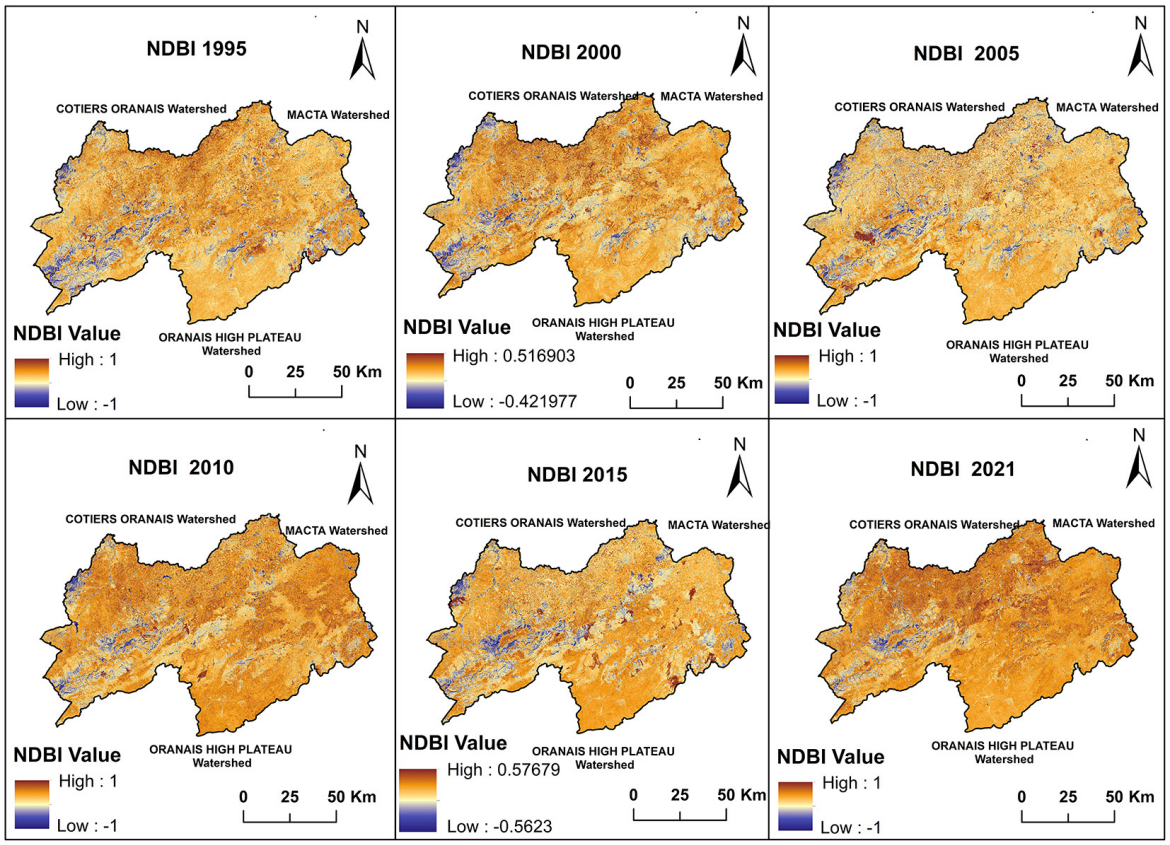

Figure 7. Spatial and temporal variation in NDBI over the period studied

built-up areas at the expense of other land covers, such as vegetation, water bodies, and bare soil, over the entire period. It should be noted that some areas showed increasing NDBI values for years 2000, 2005, 2010, 2015 and 2021, indicating a conversion of vegetated and arid lands into built-up areas during these periods, which is reflected in the high NDBI values observed. In contrast, the same areas show NDBI values higher than 0.25 for the year 1995, indicating stability in built-up areas and a high rate of bare land over this period. This indicates a clear expansion of built-up areas between 2000 and 2021 compared to 1995.

Relationship between LST and NDVI/NDBI

The results presented in (Table 5) highlight the regional landscape dynamics and the relationships between NDVI, NDBI, and LST over time. The calculated mean NDVI experienced a noticeable decrease from 0.23 in 1995 to 0.19 in 2021. Similarly, the calculated mean NDBI remained relatively stable, changing from 0.13 in 1995 to 0.12 in 2021. Conversely, the LST has trended upward, with an average ranging from 36.61 °C in 1995 to 40.35 °C in 2021. Furthermore, LST exhibited interannual variability in conjunction with NDVI and NDBI. All tested relationships between NDVI, NDBI, and LST showed statistical significance with a p-value ≤0.0001, confirming the robustness of these associations. The adjusted R-value, which measures the proportion of variance in the dependent variable LST explained by the independent variables NDVI and NDBI, reached its highest value of 0.67 in 2010, indicating a relatively strong relationship between these factors (LST-NDBI). Conversely, the lowest adjusted R value of -0.26 was observed in 2000, suggesting a weaker relationship between LST and NDVI during that specific period.

Figure 7 presents the results of the linear regression analysis on a sample of 1043 independent observation points. These observations were collected to examine the correlation between LST and the normalised indices NDBI and NDVI on an interannual level. The regression analysis shows a positive association between LST and NDBI, while it is negative between LST and NDVI. The positive relationship between LST and NDBI (Figure 8a) implies that the areas with more built-up structures tend to have higher LST, as supported by the correlation coefficients indicated in (Table 5). This situation is a result of a combination of factors that do not comply with building standards as practiced in the most advanced countries in terms of climate (urban morphology, unsuitable materials, soil impermeability, reduced green spaces, absence of water

Table 5. Statistical analysis of LST and indices (NDVI, NDBI) and their relationship

Statistics of LST and Land Indices (NDVI, NDBI)					Relationship between Land Indices and LST
Date	Variables	Minimum	Maximum	Mean	Correlation with LST (R)
28/08/1995	LST	12.36	49.56	36.61	-
	NDVI	-1	0.864	0.23	-0.52
	NDBI	-1	0.99	0.13	0.66
09/08/2000	LST	18.38	50.28	37.72	-
	NDVI	-0.32	0.77	0.19	-0.26
	NDBI	-0.42	0.51	0.14	0.47
23/08/2005	LST	15.64	47.39	37.38	-
	NDVI	-1	0.87	0.20	-0.48
	NDBI	-1	1	0.12	0.55
05/08/2010	LST	21.06	54.17	40.18	-
	NDVI	-1	0.88	0.23	-0.55
	NDBI	-1	1	0.13	0.67
18/08/2015	LST	21.17	40.22	31.76	-
	NDVI	-0.38	0.86	0.22	-0.58
	NDBI	-0.56	0.57	0.09	0.6
18/07/2021	LST	23.67	49.86	40.35	-
	NDVI	-1	1	0.2	-0.47
	NDBI	-1	1	0.12	0.65

features, etc.). Conversely, a significantly negative correlation is found between LST and NDVI, as illustrated in (Figure 8b), which confirms the hypotheses mentioned above. These findings confirm that the areas with denser vegetation cover generally have a lower LST.

Identification of drought hot spots and cold spots using NDVI, LST and VHI

To study the intensity of the thermal field, a detailed analysis of hotspots (Figure 9a, 9b) was conducted using ArcGIS software with 90%, 95%, and 99% confidence intervals. The results reveal distinct patterns of LST, characterised by high values (hotspots) and low values (cold spots), indicating increased and decreased temperature variations (Figure 9a).The cold spots are primarily located in natural reserves, including forested areas, situated to the south and northwest of Tafna, as well as in the central Macta region. Furthermore, the analysis also demonstrates a trend of expanding spatial coverage of LST hotspots from 1995 to 2021. In terms of area, the

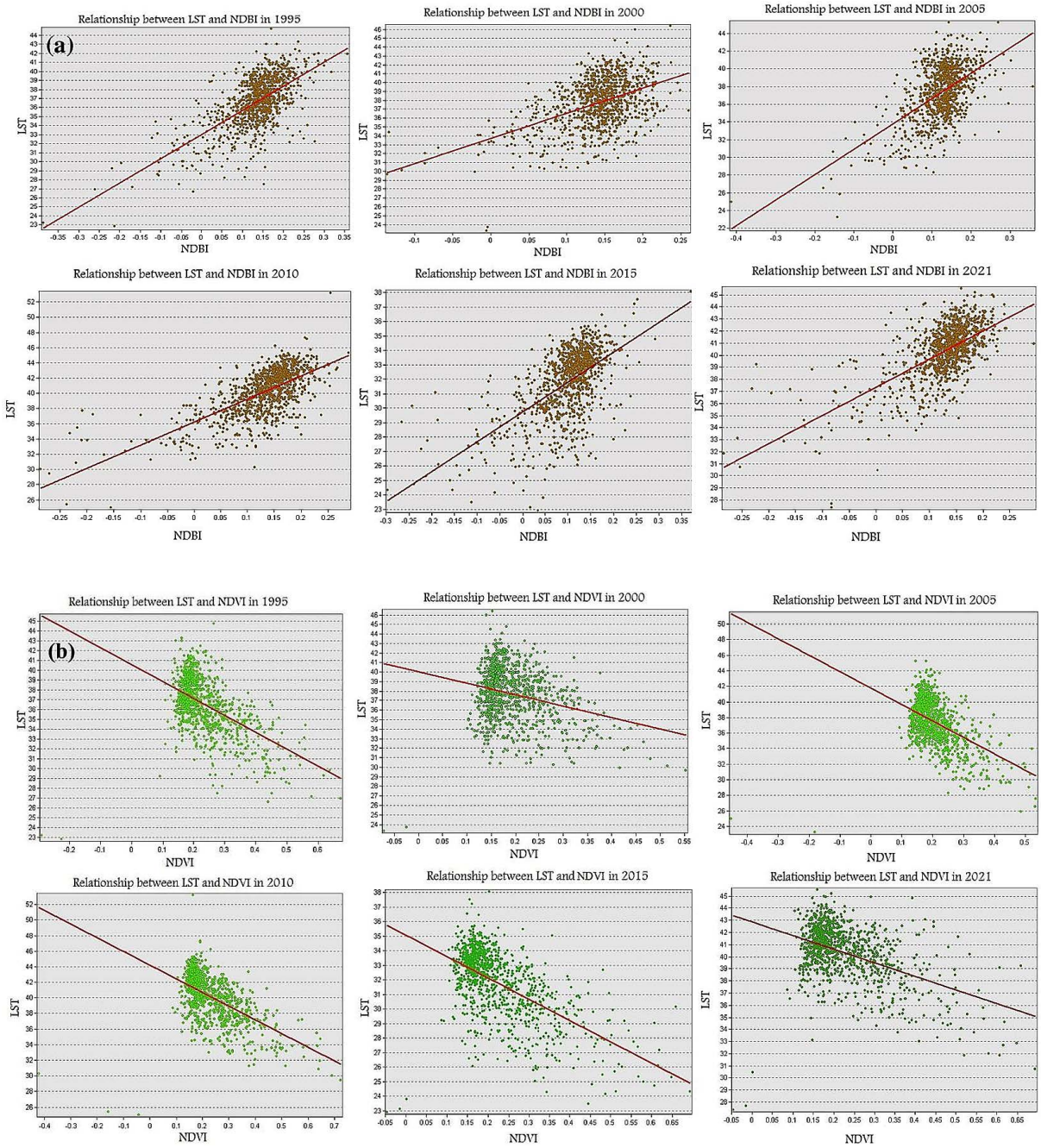

Figure 8. LST-NDBI and LST-NDVI correlation

results provide information about the increase in LST. Nonetheless, the Mediterranean region is considered one of the most vulnerable regions to climate change, characterised by a significant rise in temperatures in recent decades. This increase can be attributed to several factors, including changes in urbanisation, variations in elevation, slope, temperature fluctuations, and alterations in vegetation cover. Furthermore, an investigation into the LULC corresponding to LST hotspots and cold spots was carried out by overlaying the hotspot and cold spot layers with the LULC layers. Forest areas emerge as significant contributors to the cold spot regions (Figure 9a) and (Figure 3) of LULC. The years 2000, 2005, 2010, and 2015 stand out for the emergence of substantial

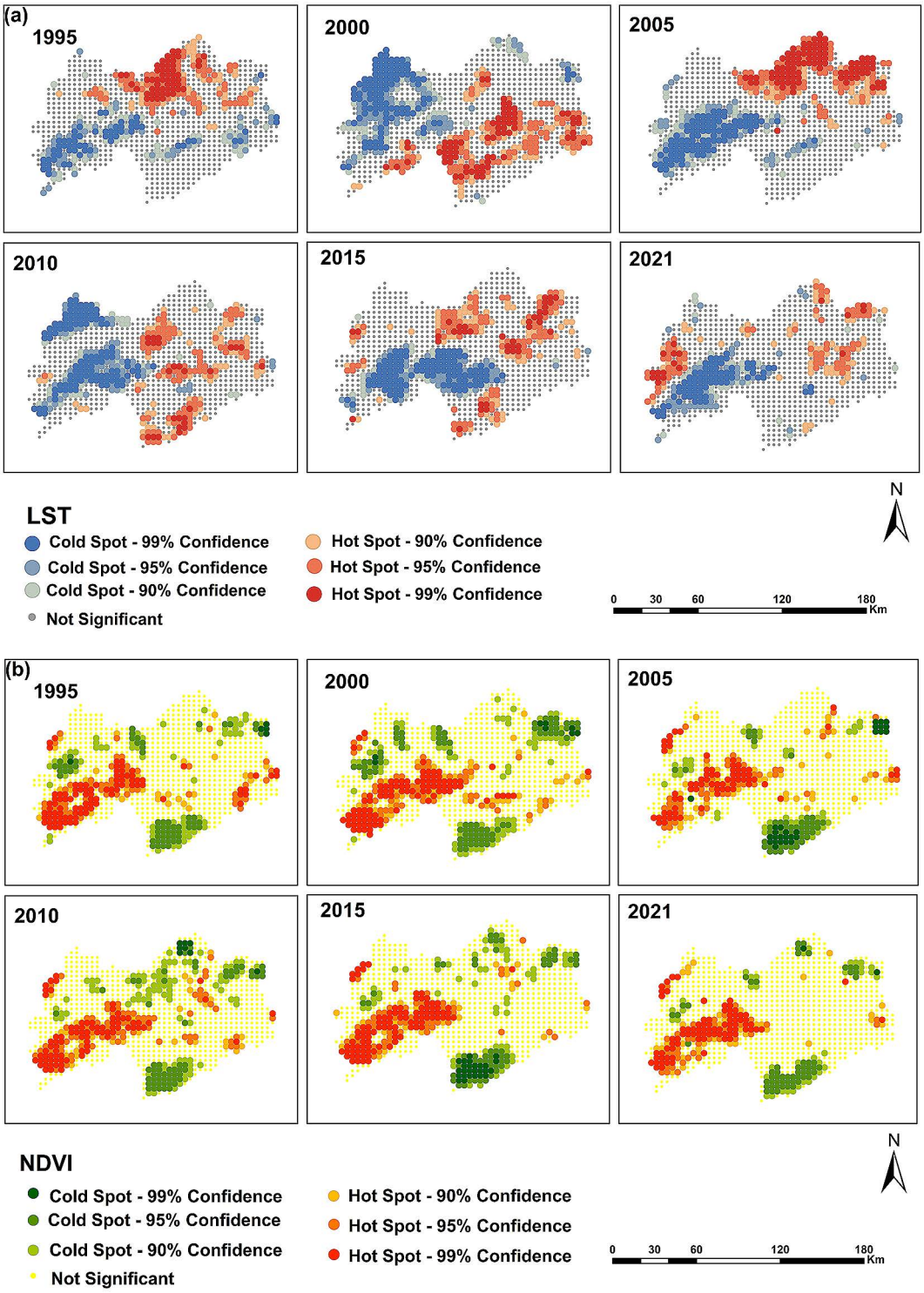

Figure 9. Mapping vulnerability to drought: hot and cold spots NDVI, LST and VHI

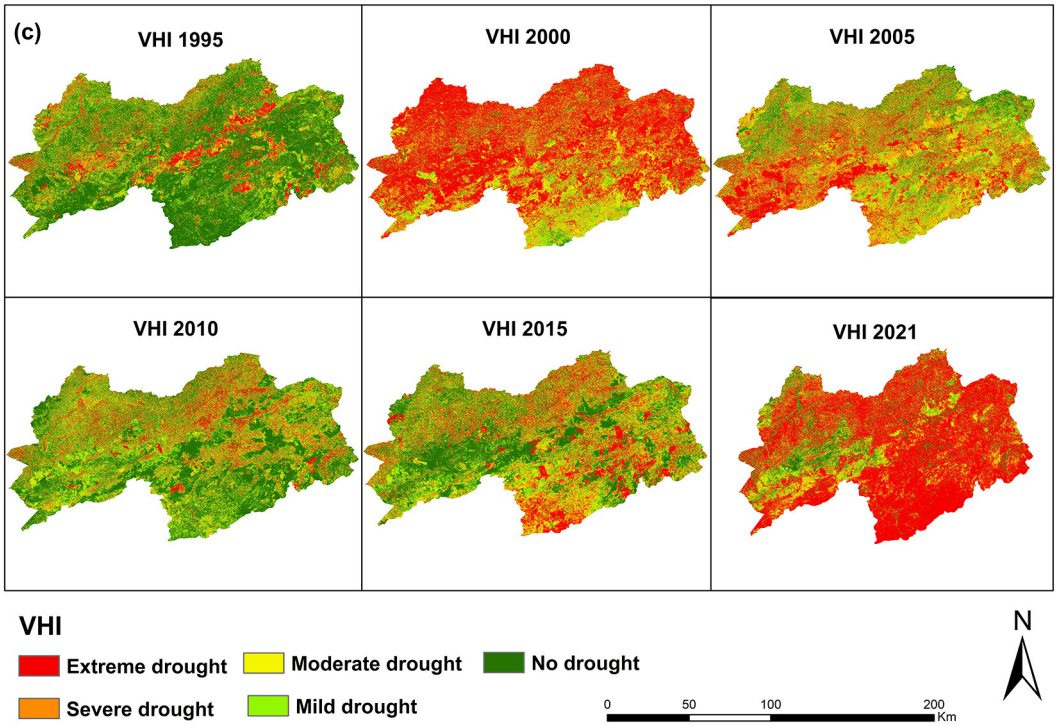

Figure 9. Cont. Mapping vulnerability to drought: hot and cold spots NDVI, LST and VHI

cold spot areas, especially in forested and cultivated zones. Conversely, LST hotspots mainly appeared in built-up land areas. In 2000, the hotspot was primarily confined to the southern part of Macta; in the following years, it gradually encompassed almost the entire northern area. It is worth noting that small, scattered water bodies in the area exhibited cooler temperatures, serving as localised cool spots. These water bodies play a central role in mitigating the urban thermal environment by providing a positive impact on temperature reduction, but within certain spatial limits. The spatial distribution of NDVI hotspots is illustrated in (Figure 9b), showing a concerning decline. Upstream of the Tafna basin, a dominant spatial pattern reveals a hotspot area of NDVI that decreases over time. In addition, three persistent cold spots are observed in the north-eastern and central parts of the Tafna basin, indicating a statistically significant decrease in vegetation cover. In the central Macta region, a band is characterised by an absence of noticeable hotspots or cold spots, suggesting the absence of explicit spatial patterns or trends in vegetation cover throughout the two-decade period. In a specific segment of the central Macta basin, a limited area exhibits oscillating hotspots, indicating declining vegetation cover from 1995 to 2015, an absence of cover in 2021, and a significant downward trend each year. Nevertheless, this region also has a historical record of low vegetation cover. On the other hand, an intensifying cold area predominates in the southern and north-eastern wings of the Macta basin, illustrating consistently low vegetation cover despite the increasingly cold characteristics of the region. The geographical area is located at the interface of Mediterranean and Saharan environmental influences. Mediterranean air masses exhibit distinctive characteristics in the form of anticyclones that result in dry summers. Saharan climatic impacts are characterised by the prevalence of north and northeast winds, which are dominant in both winter and summer. The vegetation in the north-western part of Algeria is influenced by the interaction between Saharan climatic factors and Mediterranean air masses. As shown in (Figure 9b)**,** almost the entire study area displays a statistically significant downward trend in NDVI values, indicating a general reduction in vegetation cover over the analysed period, whether in hotspots or cold spots. The integration of LST and NDVI alone may not be sufficient for a complete drought analysis. Therefore, VHI is calculated for accurate drought detection by a combination of VCI and TCI. Graphical observation of the VHI maps offers nuanced information on drought patterns and their spatial variations. This integration of

remote sensing data into climate change studies is beneficial for identifying hotspots. Figure 9c presents the VHI by providing the drought severity statement. A distinctive pattern of drought appears, with significant vegetation stress observed in 2000 and 2021, covering 52.26% and 61.04% of the area respectively. This stress is attributed to widespread vegetation growth under climatic anomalies, indicative of severe drought during these periods. Conversely, moderate drought conditions were identified, representing 22.33% in 2005 and 17.11% in 2015. In addition, it is crucial to point out that the VHI shows notable decreases in the north-west, potentially influenced by the increase in LST in this region over recent decades (Figure 9c). This interaction of observed indices and models improves the understanding of drought dynamics.

LULC and LST projections for 2030 and 2050

Figure 10 illustrates the projected scenarios for LULC and LST for the years 2030 and 2050. On the basis of the results of the conducted simulation, a notable reduction in the area of agricultural land is observed, with a decrease of 27.55% in 2030 and 27.13% in 2050, compared to the 28.21% reported in 2021 (Figure 4), followed by a decrease in bare land of 50.44% in 2030 and 50.35% in 2050, as well as a substantial increase in forested areas of 19.37% and 19.31% in 2030 and 2050, respectively (Figure 10). Furthermore, the LST projections indicate high temperatures in the central Macta region and the south and north-west of Tafna. Uncontrolled urbanisation to the north and the increasing LST trends observed in the area raise concerns for urban managers and planners. The regions where expected LST values are particularly high (Figure 10), should be a priority for implementing measures to mitigate the urban heat island (UHI) effect. Potential factors contributing to temperature increase include greenhouse effect variations, climate warming, and changes in surface characteristic.

DISCUSSION

The distribution patterns of LST and NDVI show spatially opposite characteristics (Figure 8b). The high NDVI values in the south-western parts of TAFNA and in the central MACTA coincide with relatively low LST values. This confirms the direct impact of vegetation, considered as green frame, on temperatures by effectively reducing the amount of absorbed radiation, a phenomenon demonstrated by (Zhou et al., 2017), according to which vegetation cover generally has a

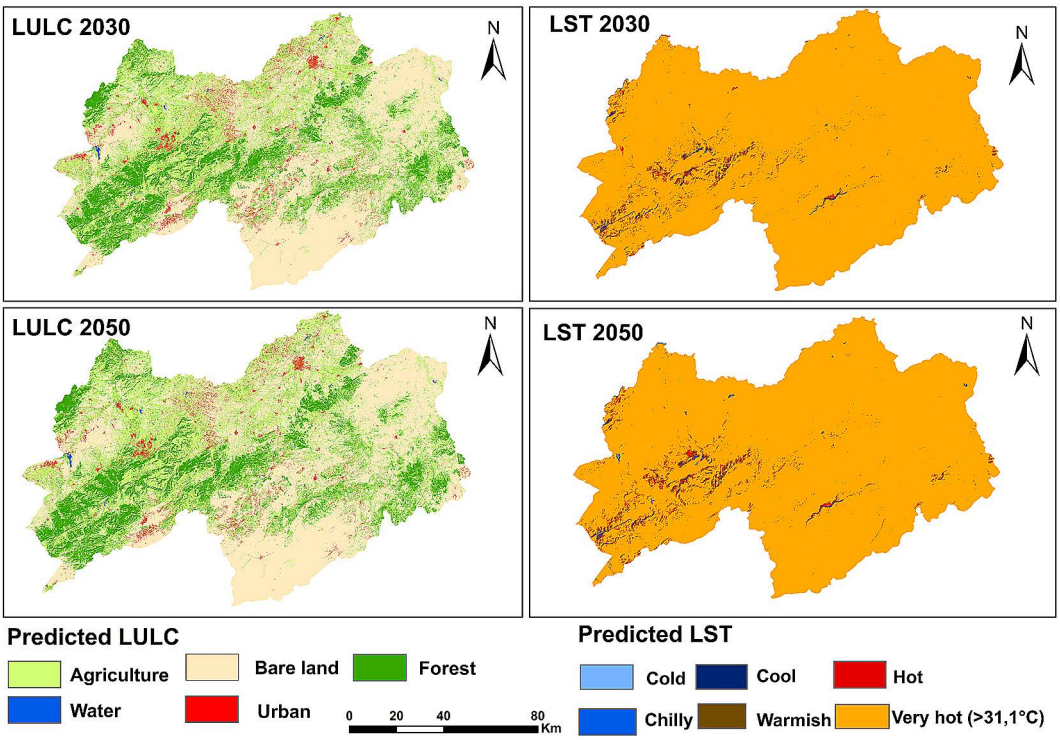

Figure 10. Forecasts for 2030 and 2050 regarding LULC and LST

moderating effect on LST. Conversely, other areas display high LST peaks with low NDVI values due to reduced shading and evapotranspiration, creating water stress and reducing the contribution of vegetation to the temperature mitigation processes. This indicates that vegetation growth and productivity can also be influenced by temperature, creating a feedback loop between NDVI and LST. The correlation results reveal a negative relationship between NDVI and LST, with statistically significant "R" values ranging from -0.52 (high), -0.26 (low), -0.48 (moderate), -0.55 (high), -0.58 (high), and -0.47 (moderate), respectively, at all-time steps. According to (Zheng et al., 2021), these negative correlations can occur when higher temperatures lead to increased soil water evaporation. This increased evaporation decreases soil moisture levels, creating the conditions of vegetation water stress, resulting in a decrease in NDVI. Guha et al. (2021) also found that a negative correlation occurs when water availability is a limiting factor for vegetation growth. These results are in line with those obtained by (Ferrelli et al., 2018; Li et al., 2021). Several factors contribute to varying degrees to the relationship between NDVI and LST in semi-arid regions. According to (Alademomi et al., 2022), limited and uneven vegetation cover in semi-arid areas contributes to increased LST by reducing albedo, limiting evapotranspiration, and reducing shading, thus explaining the strong correlation observed. The occurrence of climate phenomena caused by temperature anomalies leading to reduced precipitation in the region can also contribute to the increase in LST and the reduction of vegetation photosynthetic capacity. However, a moderate to low correlation of -0.26 between NDVI and LST is observed for the year 2000 in the study region, contradicting the results of other years. This discrepancy could be attributed to soil moisture levels, as wet conditions allow the soil to absorb more heat, resulting in lower LST values (Hussain et al., 2023). Differential soil moisture conditions can lead to variable LST estimates, even under uniform NDVI conditions (Njoku and Tenenbaum 2022). On the other hand, available rainfall data indicate that the year 2000 experienced abnormally low rainfall in the region, which would have contributed to drier soils, in turn increasing surface temperature and potentially negatively impacting vegetation, thus reducing NDVI. On the other hand, the relationship between LST and NDBI shows a moderate to high positive correlation ranging from 0.47 to 0.67. The development of LST in the region has been favoured by rapid urban growth at the expense of vegetated areas. Indeed, NDBI reflects the presence of non-vegetated surfaces, such as urban areas, roads, and bare soil, which have a warming effect on the land surface. These surfaces generally have a higher albedo (i.e., they reflect less radiation), leading to increased heat absorption and higher LST values (Zhang et al., 2017). Research on the thermo-physical properties of materials has revealed how various urban elements such as building roofs, road pavements, green spaces, and urban forests can influence the microclimatic conditions of the urban environment, especially concerning albedo (Al-Hafiz et al., 2017; Yang et al., 2015). This positive relationship confirms the predominant role in the formation of the UHI (Renard et al., 2019; Subhanil and Govil 2021). (Rashid et al., 2021) found similar findings in their studies. Changes in correlation coefficients between NDVI and LST, as well as between LST and NDBI, are attributed to a combination of interannual variations, climatic influences, land cover changes, and local factors. Moreover, the physical characteristics of semi-arid regions, such as low rainfall, strong winds, and limited cloud cover, contribute to the strong relationship between NDVI, NDBI, and LST. These conditions result in a reduction in the amount of moisture available to the ecosystem, amplifying the effects of water and thermal stress on vegetation. The impact of land cover changes has been studied by examining transitions between land cover types. The highest observed transitions were for water, built-up areas, and bare land (Figures 3 and 4).The spatial extent of agricultural land and forests has significantly decreased by 17.45% and 1.36%, respectively, between 1995 and 2021. The central and northern regions of Macta, as well as the western part of Tafna, have been more heavily affected by this regression. Overall, forest degradation is mainly related to a combination of natural and anthropogenic factors. Among these factors is climate change, such as the increasing frequency and severity of droughts in the region, forest fires, soil degradation, and the expansion of urban areas (Bentchakal et al., 2021). In addition, human activities, such as vegetation restoration and land use modifications, play a significant role in vegetation growth, resulting in various land-use characteristics (Jiang et al., 2021; Li et al., 2021). The effects of these land cover changes have repercussions on

the environmental dynamics of the region. Different land cover types exhibit varying responses to LST, NDVI, and NDBI, underscoring the importance of considering land cover in environmental assessments. Water bodies and vegetation have cooling effects on LST, while urban areas and bare soils contribute to the UHI effect, increasing diurnal LST (Alademomi et al., 2022).

Getis-Ord G* statistical results are used for drought monitoring. The analysis reveals an increasing trend in the spatial extent of LST hotspots from 1995 to 2021. This expansion is closely related to changes in LULC, characterised by unplanned urban sprawl and a reduction in cultivated lands. Uncontrolled urban expansion has adverse consequences for the environment, potentially leading to the long-term deterioration of the region (Yin et al., 2022). According to (Mosammam et al., 2017), unplanned urban sprawl could significantly harm the environment, while planned urban sprawl mitigates these adversities to a greater extent. Studies have shown that the most critical factor in urban sprawl is the presence of roads providing access to major development hotspots and other facilities (Hasan et al., 2022). The expansion of the UHI phenomenon becomes evident when evaluating changes over a 26-year period. Conversely, the cold spots in water bodies emphasise their vital role in mitigating extreme temperatures. These cooling effects on water bodies highlight their ecological importance and the need to preserve them against urbanisation pressures. On the other hand, hot and cold drought spots based on NDVI are detected upstream of the Tafna basin and in parts of Macta, indicating a decrease in vegetation cover clustering intensity. Declining hot spot proportions are increasingly observed in both basins. These results are consistent with long-term changes in LST and LULC models induced by climate change. These results highlight the importance of land conservation measures and development planning to preserve natural ecosystems and promote sustainable use of land resources. Overall, the analysis highlights the strong association between LST, NDVI and NDBI, underlying land use, and land cover conditions significantly influencing their distribution and intensity. It marks the end of a sectoral management process that allows for divergent actions and considers very little living space. The adoption of integrated, sustainable management is the best defence against the undeniable effects of climate warming that threatens citizens.

CONCLUSIONS

This study analysed the complex dynamics and interrelationships between the environmental variables NDVI, NDBI and LST in relation with land cover change and the effects of climate change at the local scale. The conducted observations have allowed assessing the magnitude as well as scope of the threats and challenges that are emerging in relation to the identified trends, taking into account climate change projections specific to the study area. The configuration and values of these three parameters vary accordingly with changes in land cover. The results demonstrate that lower NDVI values were found in the areas where LST and NDBI are higher. Furthermore, the interaction between LST and NDBI depended on specific types of LULC. The negative correlation between NDVI and LST revealed that interannual fluctuations have a significant impact on vegetation growth, with a declining trend in NDVI. On this basis, it can be concluded that there is a strong and significant interaction between these environmental variables outside periods of water stress and with a comfortable soil water reserve. The substantial transformations in LULC highlight the constant dynamic nature of changes and the impact of human activities on the landscape. The observed spatial patterns reflect the extensive conversion of previously vegetated and arid lands into urbanised or built-up areas. This expansion is attributed to various factors, including population growth, urbanisation, land development activities, and the mass exodus of people from the south forced by the continuing high temperatures that are the very expression of climate change. To better understand the spatio-temporal dynamics of LST and NDVI, the Getis-Ord-Gi* statistical analysis was employed. The results of this analysis indicate that the region has experienced simultaneous increases in LST, rapid urbanisation, and significant vegetation loss, clearly illustrating the expansion of heat islands, especially in the north and northeast of the area. The implications of this study are considerable. They underscore the crucial need for sustainable land resource management and development planning in the region. To mitigate the UHI effect and preserve natural ecosystems, policymakers and urban planners must prioritise measures such as reforestation, controlled urban growth, and water resource management. These actions cannot be undertaken in a piecemeal and sectoral manner but should be part of a sustainable and integrated approach, especially with a focus on

raising awareness. However, shortcomings have been identified, such as the lack of in-depth analysis of the impact of climate change. Future research should consider more impact factors, such as water retention capacity, groundwater variations, and soil properties, which have a significant influence on watershed development. These high-contributing factors could also be examined for predicting vegetation and LST change trends, which are essential for ecosystem development. The extraction of three factors from a significantly more extensive and complex set reveals the direct effects of climate change on populations in the southern regions, compelled to mobility and in search of the areas with a milder climate, close to the sea. However, this situation is expected to intensify and reach physical horizons previously untouched, such as groundwater, the primary water resource, which is heavily exploited for domestic needs without coherent and sustainable management.

REFERENCES

1. Abdulmana, S., Lim, A., Wongsai, S., Wongsai, N. 2021. Land surface temperature and vegetation cover changes and their relationships in Taiwan from 2000 to 2020. Remote Sens. Appl. Soc. Environ. 24, 100636. https://doi.org/10.1016/j.rsase.2021.100636
2. Akhsin, W., Nur, B., Fariz, T.R. 2024. Built-Up Development Prediction Based on Cellular Automata Modelling Around New Yogyakarta International Airport. Ecol. Eng. Environ. Technol. 25, 238–250. https://doi.org/10.12912/27197050/175138
3. Al-Hafiz, B., Musy, M., Hasan, T. 2017. A study on the impact of changes in the materials reflection coefficient for achieving sustainable urban design. Procedia Environ. Sci. 38, 562–570. https://doi.org/10.1016/j.proenv.2017.03.126
4. Alademomi, A.S., Okolie, C.J., Daramola, O.E., Akinnusi, S.A., Adediran, E., Olanrewaju, H.O., Alabi, A.O., Salami, T.J., Odumosu, J. 2022. The interrelationship between LST, NDVI, NDBI, and land cover change in a section of Lagos metropolis, Nigeria. Appl. Geomatics 14, 299–314. https://doi.org/10.1007/s12518-022-00446-y
5. Aredehey, G., Mezgebu, A., Girma, A. 2018. Land-use land-cover classification analysis of Giba catchment using hyper temporal MODIS NDVI satellite images. Int. J. Remote Sens. 39, 810–821. https://doi.org/10.1080/01431161.2017.1392639
6. Atayi, J., Kabo-Bah, A., Akpoti, K. 2016. The effects of large-scale mining on land use and land cover changes using remotely sensed data 1. Int. J. Sci. Nat. 7, 724–733.
7. Ayad, N.A., Ayad, A.A., Khalidi, K., El, Habib, A., Charif, A. 2023. Remote Sensing and Meteorological Indexes of Drought Using Open Short Time-Series Data in Doukkala Region , Morocco. Ecol. Eng. Environ. Technol. Technol. 24, 1–10. https://doi.org/10.12912/27197050/156962
8. Bentchakal, M., Medjerab, A., Chibane, B., Rahmani, S.E.A. 2021. Meteorological drought and remote sensing data: An approach to assess fire risks in the Algerian forest. Model. Earth Syst. Environ. 1–12. https://doi.org/10.1007/s40808-021-01323-0
9. Bhatti, S.S., Tripathi, N.K. 2014. Built-up area extraction using Landsat 8 OLI imagery. GIScience Remote Sens. 51, 445–467. https://doi.org/10.1080/15481603.2014.939539
10. Edan, M.H., Maarouf, R.M., Hasson, J. 2021. Predicting the impacts of land use/land cover change on land surface temperature using remote sensing approach in Al Kut, Iraq. Phys. Chem. Earth 123, 103012. https://doi.org/10.1016/j.pce.2021.103012
11. Fayech, D., Tarhouni, J. 2021. Climate variability and its effect on normalized difference vegetation index (NDVI) using remote sensing in semi-arid area. Model. Earth Syst. Environ. 7, 1667–1682. https://doi.org/10.1007/s40808-020-00896-6
12. Feizizadeh, B., Omarzadeh, D., Kazemi Garajeh, M., Lakes, T., Blaschke, T. 2023. Machine learning data-driven approaches for land use/cover mapping and trend analysis using Google Earth Engine. J. Environ. Plan. Manag. 66, 665–697. https://doi.org/10.1080/09640568.2021.2001317
13. Ferrelli, F., Huamantinco Cisneros, M.A., Delgado, A.L., Piccolo, M.C. 2018. Spatial and temporal analysis of the LST-NDVI relationship for the study of land cover changes and their contribution to urban planning in Monte Hermoso, Argentina. https://doi.org/10.5565/rev/dag.355
14. Ghobadi, Y., Pradhan, B., Shafri, H.Z.M., Kabiri, K. 2015. Assessment of spatial relationship between land surface temperature and landuse/cover retrieval from multi-temporal remote sensing data in South Karkheh Sub-basin, Iran. Arab. J. Geosci. 8, 525–537. https://doi.org/10.1007/s12517-013-1244-3
15. Guha, S., Govil, H., Gill, N., Dey, A. 2021. A long-term seasonal analysis on the relationship between LST and NDBI using Landsat data. Quat. Int. 575, 249–258. https://doi.org/10.1016/j.quaint.2020.06.041
16. Hasan, M., Hassan, L., Al, M.A., Abualreesh, M.H., Idris, M.H., Kamal, A.H.M. 2022. Urban green space mediates spatiotemporal variation in land surface temperature: a case study of an urbanized city, Bangladesh. Environ. Sci. Pollut. Res. 29, 36376–36391. https://doi.org/10.1007/s11356-021-17480-9
17. Hussain, S., Mubeen, M., Ahmad, A., Akram, W., Hammad, H.M., Ali, M., Masood, N., Amin, A., Farid, H.U., Sultana, S.R. 2020. Using GIS tools

to detect the land use/land cover changes during forty years in Lodhran District of Pakistan. Environ. Sci. Pollut. Res. 27, 39676–39692. https://doi.org/10.1007/s11356-019-06072-3

18. Hussain, S., Raza, A., Abdo, H.G., Mubeen, M., Tariq, A., Nasim, W., Majeed, M., Almohamad, H., Al Dughairi, A.A. 2023. Relation of land surface temperature with different vegetation indices using multi-temporal remote sensing data in Sahiwal region, Pakistan. Geosci. Lett. 10. https://doi.org/10.1186/s40562-023-00287-6
19. IPCC. 2022. Climate Change 2022 - Mitigation of Climate Change - Full Report, Cambridge University Press.
20. Jiang, L., Liu, Y., Wu, S., Yang, C. 2021. Analyzing ecological environment change and associated driving factors in China based on NDVI time series data. Ecol. Indic. 129, 107933. https://doi.org/10.1016/j.ecolind.2021.107933
21. Keerthi Naidu, B.N., Chundeli, F.A. 2023. Assessing LULC changes and LST through NDVI and NDBI spatial indicators: a case of Bengaluru, India. GeoJournal 88, 4335–4350. https://doi.org/10.1007/s10708-023-10862-1
22. Kumari, B., Tayyab, M., Shahfahad, Salman, Mallick, J., Khan, M.F., Rahman, A. 2018. Satellite-driven land surface temperature (LST) using Landsat 5, 7 (TM/ETM+ SLC) and Landsat 8 (OLI/TIRS) data and its association with built-up and green cover over urban Delhi, India. Remote Sens. Earth Syst. Sci. 1, 63–78. https://doi.org/10.1007/s41976-018-0004-2
23. Lhissou, R., El Harti, A., Maimouni, S., Adiri, Z. 2020. Assessment of the image-based atmospheric correction of multispectral satellite images for geological mapping in arid and semi-arid regions. Remote Sens. Appl. Soc. Environ. 20, 100420. https://doi.org/10.1016/j.rsase.2020.100420
24. Li, P., Wang, J., Liu, M., Xue, Z., Bagherzadeh, A. 2021. Spatio-temporal variation characteristics of NDVI and its response to climate on the Loess Plateau from 1985 to 2015. Catena 203, 105331. https://doi.org/10.1016/j.catena.2021.105331
25. Li, S., Xu, L., Jing, Y., Yin, H., Li, X., Guan, X. 2021. International Journal of Applied Earth Observations and Geoinformation High-quality vegetation index product generation : A review of NDVI time series reconstruction techniques. Int. J. Appl. Earth Obs. Geoinf. 105, 102640. https://doi.org/10.1016/j.jag.2021.102640
26. Macarof, P., Statescu, F. 2017. Comparasion of NDBI and NDVI as indicators of surface urban heat island effect in landsat 8 imagery: a case study of Iasi. Present Environ. Sustain. Dev. 141–150. https://doi.org/10.1515/pesd-2017-0032
27. Malik, M.S., Shukla, J.P., Mishra, S. 2019. Relationship of LST, NDBI and NDVI using landsat-8 data in Kandaihimmat watershed, Hoshangabad, India. Indian J. Geo Mar. Sci.
28. Masson-Delmotte, V.P., Zhai, P., Pirani, S.L., Connors, C., Péan, S., Berger, N., Caud, Y., Chen, L., Goldfarb, M.I., Scheel Monteiro, P.M. 2021. Ipcc, 2021: Summary for policymakers. in: Climate change 2021: The physical science basis. contribution of working group i to the sixth assessment report of the intergovernmental panel on climate change. https://doi.org/doi:10.1017/9781009157896.001
29. Mehmood, M.S., Rehman, A., Sajjad, M., Song, J., Zafar, Z., Shiyan, Z., Yaochen, Q. 2023. Evaluating land use/cover change associations with urban surface temperature via machine learning and spatial modeling: Past trends and future simulations in Dera Ghazi Khan, Pakistan. Front. Ecol. Evol. 11, 1–16. https://doi.org/10.3389/fevo.2023.1115074
30. Mosammam, H.M., Nia, J.T., Khani, H., Teymouri, A., Kazemi, M. 2017. Monitoring land use change and measuring urban sprawl based on its spatial forms: The case of Qom city. Egypt. J. Remote Sens. Sp. Sci. 20, 103–116. https://doi.org/10.1016/j.ejrs.2016.08.002
31. Müller, L.M., Bahn, M. 2022. Drought legacies and ecosystem responses to subsequent drought. Glob. Chang. Biol. 28, 5086–5103. https://doi.org/10.1111/gcb.16270
32. Naserikia, M., Asadi Shamsabadi, E., Rafieian, M., Leal Filho, W. 2019. The urban heat island in an urban context: A case study of Mashhad, Iran. Int. J. Environ. Res. Public Health 16, 313. https://doi.org/10.3390/ijerph1603031
33. Njoku, E.A., Tenenbaum, D.E. 2022. Quantitative assessment of the relationship between land use/land cover (LULC), topographic elevation and land surface temperature (LST) in Ilorin, Nigeria. Remote Sens. Appl. Soc. Environ. 27, 100780. https://doi.org/10.1016/j.rsase.2022.100780
34. Policelli, F., Hubbard, A., Jung, H.C., Zaitchik, B., Ichoku, C. 2018. Lake Chad total surface water area as derived from land surface temperature and radar remote sensing data. Remote Sens. 10, 252. https://doi.org/10.3390/rs10020252
35. Purwanto, Utomo, D.H., Kurniawan, B.R. 2016. Spatio Temporal Analysis Trend of Land Use and Land Cover Change Against Temperature Based on Remote Sensing Data in Malang City. Procedia - Soc. Behav. Sci. 227, 232–238. https://doi.org/10.1016/j.sbspro.2016.06.066
36. Rani, N., Mandla, V.R., Singh, T. 2017. Evaluation of atmospheric corrections on hyperspectral data with special reference to mineral mapping. Geosci. Front. 8, 797–808. https://doi.org/10.1016/j.gsf.2016.06.004
37. Rashid, K.J., Hoque, M.A., Esha, T.A., Rahman, M.A., Paul, A. 2021. Spatiotemporal changes of vegetation and land surface temperature in the

refugee camps and its surrounding areas of Bangladesh after the Rohingya influx from Myanmar. Environ. Dev. Sustain. 23, 3562–3577. https://doi.org/10.1007/s10668-020-00733-x

38. Renard, F., Alonso, L., Fitts, Y., Hadjiosif, A., Comby, J. 2019. Evaluation of the effect of urban redevelopment on surface urban heat islands. Remote Sens. 11, 299. https://doi.org/10.3390/rs11030299
39. Rossi, F., Becker, G. 2019. Creating forest management units with Hot Spot Analysis (Getis-Ord Gi*) over a forest affected by mixed-severity fires. Aust. For. 82, 166–175. https://doi.org/10.1080/00049158.2019.1678714
40. Roy, A., Inamdar, A.B. 2019. Multi-temporal Land Use Land Cover (LULC) change analysis of a dry semi-arid river basin in western India following a robust multi-sensor satellite image calibration strategy. Heliyon 5. https://doi.org/10.1016/j.heliyon.2019.e01478
41. Santos, J.Y.G. dos, Montenegro, S.M.G.L., Silva, R.M. da, Santos, C.A.G., Quinn, N.W., Dantas, A.P.X., Ribeiro Neto, A. 2021. Modeling the impacts of future LULC and climate change on runoff and sediment yield in a strategic basin in the Caatinga/Atlantic forest ecotone of Brazil. Catena 203. https://doi.org/10.1016/j.catena.2021.105308
42. Shahfahad, Kumari, B., Tayyab, M., Ahmed, I.A., Baig, M.R.I., Khan, M.F., Rahman, A. 2020. Longitudinal study of land surface temperature (LST) using mono-and split-window algorithms and its relationship with NDVI and NDBI over selected metro cities of India. Arab. J. Geosci. 13, 1–19. https://doi.org/10.1007/s12517-020-06068-1
43. Sharma, R., Chakraborty, A., Joshi, P.K. 2015. Geospatial quantification and analysis of environmental changes in urbanizing city of Kolkata (India). Environ. Monit. Assess. 187, 1–12. https://doi.org/10.1007/s10661-014-4206-7
44. Somayajula, V.K.A., Ghai, D., Kumar, S. 2021. Land Use/Land Cover Change Analysis using NDVI, PCA, In: 2021 5th International Conference on Computing Methodologies and Communication (ICCMC). IEEE, 849–855. https://doi.org/10.1109/ICCMC51019.2021.9418025
45. Subhanil, G., Govil, H. 2021. Relationship between land surface temperature and normalized difference water index on various land surfaces: A seasonal analysis. Int. J. Eng. Geosci. 6, 165–173. https://doi.org/10.26833/ijeg.821730
46. Sudhakar, C.V., Reddy, G.U. 2022. Land use Land cover change Assessment at Cement Industrial area using Landsat data-hybrid classification in part of YSR Kadapa District, Andhra Pradesh, India. Int. J. Intell. Syst. Appl. Eng. 10, 75–86. https://doi.org/10.18201/ijisae.2022.270
47. Tayeb, S.T., Kheloufi, B. 2019. Spatio-temporal dynamics of vegetation cover in North-West Algeria using remote sensing data. Polish Cartogr. Rev. 51, 117–127. https://doi.org/10.2478/pcr-2019-0009
48. Yang, J., Wang, Z.-H., Kaloush, K.E. 2015. Environmental impacts of reflective materials: Is high albedo a 'silver bullet'for mitigating urban heat island? Renew. Sustain. Energy Rev. 47, 830–843. https://doi.org/10.1016/j.rser.2015.03.092
49. Yin, S., Liu, J., Han, Z. 2022. Relationship between urban morphology and land surface temperature — A case study of Nanjing City. PLoS One 17, 1–17. https://doi.org/10.1371/journal.pone.0260205
50. Yonaba, R., Koïta, M., Mounirou, L.A., Tazen, F., Queloz, P., Biaou, A.C., Niang, D., Zouré, C., Karambiri, H., Yacouba, H. 2021. Spatial and transient modelling of land use/land cover (LULC) dynamics in a Sahelian landscape under semi-arid climate in northern Burkina Faso. Land use policy 103, 105305. https://doi.org/10.1016/j.landusepol.2021.105305
51. Zeng, J., Zhang, R., Qu, Y., Bento, V.A., Zhou, T., Lin, Y., Wu, X., Qi, J., Shui, W., Wang, Q. 2022. Improving the drought monitoring capability of VHI at the global scale via ensemble indices for various vegetation types from 2001 to 2018. Weather Clim. Extrem. 35, 100412.
52. Zeren Cetin, I., Varol, T., Ozel, H.B., Sevik, H. 2023. The effects of climate on land use/cover: a case study in Turkey by using remote sensing data. Environ. Sci. Pollut. Res. 30, 5688–5699. https://doi.org/10.1007/s11356-022-22566-z
53. Zhang, X., Wang, D., Hao, H., Zhang, F., Hu, Y. 2017. Effects of land use/cover changes and urban forest configuration on urban heat islands in a loess hilly region: case study based on Yan'an City, China. Int. J. Environ. Res. Public Health 14, 840. https://doi.org/10.3390/ijerph14080840
54. Zheng, Y., Tang, L., Wang, H. 2021. An improved approach for monitoring urban built-up areas by combining NPP-VIIRS nighttime light, NDVI, NDWI, and NDBI. J. Clean. Prod. 328, 129488. https://doi.org/10.1016/j.jclepro.2021.129488
55. Zhou, Y., Xiao, X., Zhang, G., Wagle, P., Bajgain, R., Dong, J., Jin, C., Basara, J.B., Anderson, M.C., Hain, C. 2017. Quantifying agricultural drought in tallgrass prairie region in the US Southern Great Plains through analysis of a water-related vegetation index from MODIS images. Agric. For. Meteorol. 246, 111–122. https://doi.org/10.1016/j.agrformet.2017.06.007